

CRYOMODULE DESIGN, ASSEMBLY AND ALIGNMENT

Carlo Pagani and Paolo Pierini
University of Milano and INFN Milano LASA

Abstract

In this tutorial the functions performed by superconducting RF cavity cryomodules are reviewed and the main design criteria are outlined.

THE COLD MASS: CAVITIES ET ALIA

An RF cavity cryomodule needs to provide the structural support and the cryogenic environment for one (or more) RF cavities (and their ancillary components, as frequency tuners, fundamental and high order mode couplers), in order to allow their operation at design specifications. The ensemble of devices to which a stable cryogenic environment needs to be guaranteed is usually referred as the **cold mass**. The cold mass itself is a system which follows a complex design optimization which depends on the application for which the accelerator is designed. In particular, the type and energy range of accelerated particles, and the beam current and quality goals, together with the design accelerating gradient and RF duty cycle are amongst the most influential parameters for the cold mass design.

The accelerated particle type (and energy for the case of protons and ions, for which a variety of structure geometries exist) determines the cavity shape and geometry. Beam current plays a major role on the design details of ancillaries (e.g. fundamental and high order mode couplers), and beam quality requirements can further constraint the design of them (e.g. HOM damping). The RF frequency and cavity fabrication technology determines the operating temperature, whether it is the atmospheric pressure He boiling point or the low pressure superfluid He below the lambda point.

High gradient pulsed operation requires to add a fast tuning action to the cavity mechanical tuner to dynamical control the cavity frequency, whereas CW operation with a high external Q value requires to address the issue of cold mass vibrations (the “microphonics”) with the potential of inducing large phase and amplitude oscillations of the cavity accelerating voltage.

Other machine dependent requirements can drive the cold mass design, like the necessity of a high filling factor to maximize the real estate gradient.

Due to these considerations, one can easily understand that no single technical solution can be devised to efficiently cope with the variety of cold mass configurations that can come out of this complex process. Furthermore, the cold mass needs interfaces to the ambient world, in form of RF power from the amplifiers, RF signals for control, HOM power to dissipate at appropriate locations, electrical feeds for motors and actuators. The number and sizes of these cables and devices is strongly dependent on the application for which the accelerator is designed.

However, superconducting accelerators have been built in the past thirty years, and it is worth reviewing the main technical solutions that were adopted in the past, in order to comment the current trends in cryomodules design.

CRYOMODULE DESIGN: PAST EXPERIENCE AND CURRENT TRENDS

In the past, for many SRF linac projects, the cryomodules almost followed an independent design procedure, which had aim to deliver a cryostat to contain the cold mass with minimal thermal losses. On the contrary, new generation cryomodules are more and more integrated in the process of overall design and optimization of the accelerator, starting from its conceptual stage. The cryomodule, from the point of view of the design optimization, is indeed regarded as a single entity, a cryostat containing a cold mass. Furthermore, it is one important element of the overall cryogenic system.

Indeed for a given SRF accelerator the overall cryomodule costs and performances are dominant with respect to that of any of its individual components

Components and system reliability, together with requirements for the accelerator availability to experiments, are concepts that are now included in the large accelerator design since its early stages. These new requirements determined the introduction of redundancy criteria in order to maximize the Mean Time Between Failures (MTBF) while not increasing the Mean Time To Repair (MTTR), that is usually dominated by external factors, as tunnel access or warmup and cooldown times in the worst cases of repairs inside the module itself.

Heavy ions, the early stages and future plans

Heavy ion machines, like ATLAS at ANL [1], the heavy ion linac in JAERI [2] and ALPI at LNL[3], using quarter wave SRF resonators, designed cryostats in which cavities were grouped in order to improve the machine filling factor and containing the costs. A figure of the ATLAS and ALPI cold mass are shown in Figs 1 and 2.



Figure 1: The ATLAS injector cold mass.

The moderate gradients and beam quality specifications arising from for the machine design did not require clean room assembly procedures, and did not justify a need for the physical separation between the beam vacuum environment and the cryostat isolation vacuum. This, however, limited the use of multilayer insulation (MLI) to reduce heat losses, in order to avoid beam vacuum degradation. The cavities in the cryostats are then cooled to 4.2 K through liquid He reservoirs on top. Liquid nitrogen shields are used to reduce the consumption of LHe. Finally, the cryostats do not contain magnetic elements. The cryostats devised for these structures proved to be an efficient and cost effective solution for the proposed applications.



Figure 2: The cold mass of ALPI at INFN/LNL.

Recently, considering the potential (and industrial perspectives as well) of high current-low energy SRF CW applications, a proton/deuteron linac cryomodule containing six half-wave resonators (HWRs) and magnetic focussing elements has been developed by industry (ACCEL), for an evaluation of its possible industrialization [4]. The separation of beam vacuum from the isolation vacuum has been integrated into the design, as shown in Fig. 3.

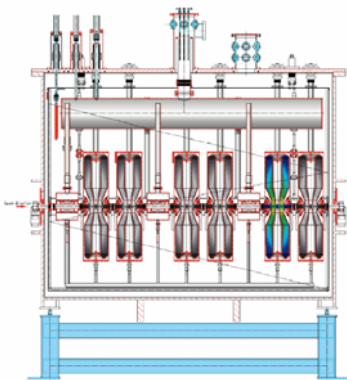


Figure 3: The ACCEL design for a HWR linac.

The RIA/ATLAS upgrade cryomodules design is another step at introducing modern features in this concept. It features vacuum separation, and clean room assembly of the cold mass.

A big change: The large projects impact in SRF Technology (LEP, HERA, CEBAF, ...)

In 1985 the successful test of a pair of SC cavities in Cornell opened the door to the large scale application of SRF for electrons. [5]

The decision of applying this (at the time) unusual technology in the largest HEP accelerators [6,7] forced the laboratories to invest heavily in R&D activities, infrastructures and quality control and quality assurance (QC & QA) techniques. The large production need of the projects (hundreds of resonators) forced the Institutions to transfer the cavity production at industries, which committed to high quality standards via consolidated QC/QA procedures.

The activities sponsored through the huge projects pushed R&D and basic research on SRF in many research groups distributed worldwide.

The main consequences of this new “era” in the SRF community on the cryomodule concept are due to the establishment of QC/QA procedures in the cavity fabrication and handling, needed to guarantee the relatively high (at the time) design gradients (around 5 MV/m).

In order to preserve the surface cleanliness at proper level, the insulation vacuum was separated from the beam vacuum. The cavity string assembly operation were started to be performed in dedicated clean rooms, and the cavity treatments and handling required large dedicated infrastructures (for chemical treatments, clean rooms, etc.). Cost-driven issues were introduced in the component design, which lead to introduce the concept of long cryo-strings, i.e. the cryogenic connection of a number of identical cryomodules, in order to minimize the number of cold/warm transitions.

The LEP II cryomodule (consisting of four units containing a single cavity connected to each other) concept is shown in Figure 4. Here, due to the simplicity of operation at 4.5 K and taking advantage of the high thermal conductivity of the cavities (Nb sputtered on Cu), an easy-access solution was preferred, with a “wrap-up” vacuum vessel. This proved to be a fortunate decision when all the cables connecting the two cavity antennas to the RF controls out of the module had to be replaced due to their failure, induced by HOM.

The CEBAF production and installation experience was crucial to establish procedures for the efficient production, successful treatment and reliable operation levels for the 2 K 1.5 GHz cavities.

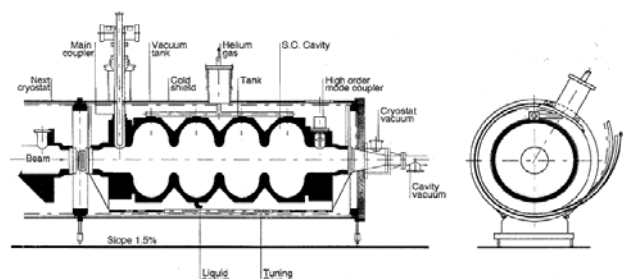


Figure 4: The CERN cryostat/module concept.

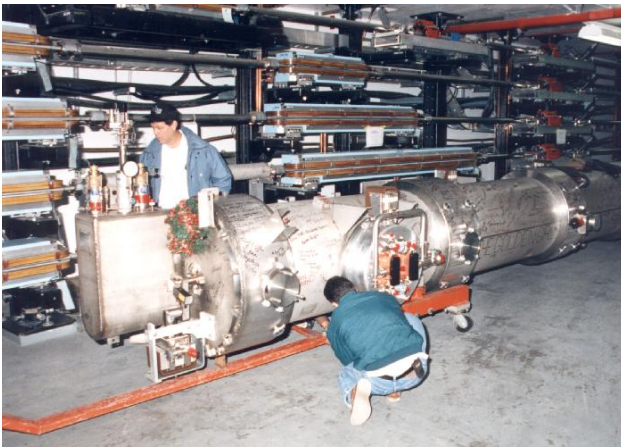


Figure 5: CEBAF modules installation in tunnel.

The TTF/TESLA Cryomodule

Another big leap in the SRF technology, and in the evolution of the cryomodule concept, has been performed with the TESLA program for the Linear Collider, and the construction and operation of its test facility, TTF (shown in Fig. 6). [8]

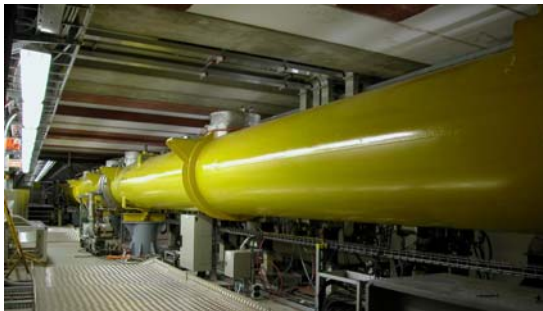


Figure 6: Modules 4 and 5 in the TTF at DESY.

One of the primary objectives of the TTF collaboration was to set a new level in the reliable operation of multicell elliptical superconducting cavities. The original goal to provide 8-cavity modules operating at 15 MV/m was outperformed, and the baseline goal was soon updated to 25 MV/m.

However, in addition to the reliable production of high gradient cavities, a high performance cryomodule was a central objective for the TESLA Mission [8,9]. More than one order of magnitude was needed to be gained in term of capital and operational cost of a 2 K superconducting machine, and this requirement called for a “new generation” cryomodule.

To fulfil the objective of the practical realization of a TeV Linear Collider a high filling factor was crucial in order to maximize the real estate accelerating gradient. This resulted in a modular design, with long subunits (cryomodules) containing many cavities (and transversely focussing elements) which could be connected together in longer strings, along the same cryogenic line.

These requirements, intended to minimize the footprint of the LC, needed to be achieved with a low cost per meter, in view of a TeV collider of several tens of kilometre length.

The considerations expressed above in terms of filling factor and costs led to an integration of the cooling and return pipes, and all the cryogenic distribution lines, into the cryomodule. The use of expensive special components or materials was also kept to the minimum possible.

Furthermore, due to the moderate duty cycle of the accelerator and its length, it was mandatory to achieve very low static losses, especially at the 2 K level, and this again was a strong motivation to minimize the number of cold to warm transitions.

Other specifications originated from the necessity to fulfil beam dynamics requirements on alignment and tolerances. The module had to be easily aligned in warm condition and needed to preserve a stable environment when brought to operation.

CRYOMODULE DESIGN CRITERIA (TAKING THE TTF MODULES AS A DESIGN EXAMPLE)

Here we discuss how the TTF module requirements briefly exposed in the previous section were fulfilled through two design iterations, during the fabrication, commissioning and operation of the TTF linac, and we illustrate the design criteria used for the conception [8,9].

The mechanical and thermal requirements

The TTF modules were originally conceived to fulfil the requirements of a TESLA cryogenic string (originally consisting of 12 modules in a subsection with individual endcaps and 12 subsections per cryoplat, for a length of 1880 m). Each TTF cryostat contains 8 cavities and one quadrupole package, for a length of approximately 12 meters. The assumed modular sectioning led to the specifications for the static heat loads for the various He circuits in each cryomodule, summarized in Table 1.

Table 1: Design estimated heat losses in the 12 m module.

Temperature	[W]	[W/m]
~ 2 K	<3	<0.25
4.5 K	<15	<1.25
~ 70 K	<90	<7.5

The driving concept behind the heat loss budget in Table 1 is that power deposition at low temperatures requires a much higher quantity of work at room temperature, due to the efficiencies of the Carnot cycle and of the thermal machine. In practice, the conversion to room temperature cooling power is 800 W/W at 2 K, 250 W/W at 4.5 K, 25-14 W/W in the range from 40 to 70 K.

Furthermore, this design philosophy implied the inclusion of the He pipes for the entire ~ 2 km cryogenic line into the transverse cross section of the cryomodule, in addition to the pipes serving the cold mass and thermal shields in each subsection. This original sectioning has been later slightly revised in the TESLA TDR, which envisaged a single cryogenic string of 2.5 km, and is still under optimization for the ILC design.

The cross section of the TTF cryomodule, contained in a 38" carbon steel vessel, is shown in Figure 6 [10,11].

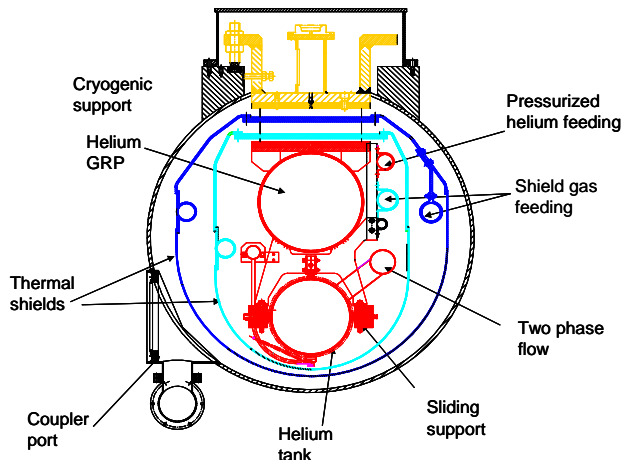


Figure 6: Cross section of the TTF cryomodule, with the description of the main components.

Each cavity is enclosed in a Ti Helium vessel, fed by the 2 K two phase supply line which returns the evaporated cold gas in the large (300 mm internal diameter) Gas Return Pipe (GRP) at each module interconnection. The GRP, which collects the low pressure 2 K He gas from the cavities in the cryogenic string and returns it to the cryoplant, acts as the structural “backbone” of the cryomodule cold mass (quadrupole package, cavity and ancillaries) and thermal shields, and is suspended to the room temperature vacuum vessel (inner diameter of ~ 950 mm) by means of composite support posts. Two Al shields at 4.5 and ~70 K, with a perimeter of 2.3 m and 2.65 m, are used for heat interception and thermal radiation shielding.

The cold active elements are suspended to the He GRP through welded brackets and longitudinal sliding supports, which allow the compensation of the differential thermal contraction of the different metals (see Table 2). This solution has been introduced in the 3rd generation cryomodule to allow a semi rigid coupler solution, while in the previous schemes the coupler had to be flexible enough to allow a maximum longitudinal cavity port displacement of approximately 15 mm with respect to the port located to the vacuum vessel.

Table 2: Total thermal contraction from 300 K to 2 K, for various materials in the module.

Material	$(L_{300}-L_2)/L_{300}$
Nb	0.146%
Ti	0.159%
Stainless Steel (304)	0.310%
Al 6061	0.419%
Invar	0.038%
G10 composite	0.274%

Three suspensions posts are used to connect the cold mass to the vacuum vessel. The central post is screwed to

the vessel, while the two other at each end can slide in order to accommodate the differential shrinkage between the room temperature vacuum vessel and the He GRP. Invar rods run along the GRP and provide reference fixed points for defining the cavity coupler position in the 3rd generation cryomodules.

The He distribution lines have been integrated within the cryomodule, and these are: the pressurized 2 K He line that is needed to cool the downstream modules, the 2 K two-phase line that supplies the saturated bath to the cavities, the 4.5 K and 70 K feed lines, the 4.5 K and 70 K return lines used for shield cooling, and a line used for cavity cooldown and warmup.

Static loads

The static loads at the different temperatures originate from two contributions: **thermal radiation** from the “hotter” environment and **direct thermal conduction** through the cold mass supports and the feedthroughs bringing components from the room temperature environment (fundamental and HOM couplers, cables, ...). The cryomodule for an RF linac needs many feedthroughs (in order to bring RF power, signals for the RF control system, sensors, tuner actuators, ...) which need to be properly taken into account and intercepted at various temperatures in order to limit their contribution to static loads.

Thermal design: thermal shielding

Due to the large number of thermal conduction paths to the 2 K cold mass, it was soon decided for the TESLA/TTF case to introduce a 4.5 K (nominal temperature, in practice 4.5 to 9 K along the string) thermal shield in order to suppress the radiation load from the environment enclosing the cold mass. We remind, in fact, that the heat flux density due to radiation transport between two surfaces at different temperatures can be written as:

$$\dot{q} = \sigma_{sb} \epsilon_{12} (T_2^4 - T_1^4)$$

where $\sigma_{sb}=5.67 \cdot 10^{-8}$ is the Stefan-Boltzmann constant and ϵ_{12} is the effective emissivity of the two surfaces, taking into account the view factor and surface emissivities. For a simple “feeling” of the order of magnitudes, it is useful to refer to the simple case of black body radiation (unitary emissivity) intercepted by a unitary surface at 2 K from a parallel plate at different temperatures, tabulated in Table 3.

Table 3: Black body radiation insisting on a 2 K surface from a parallel surface at different temperatures.

Temperature	Specific heat flux [W/m ²] at 2 K
300 K	460 W/m ²
70 K	1.4 W/m ²
4.5 K	22 10^{-6} W/m ²

From the numbers listed above it is clear that a great effort should be made to avoid any room temperature surface to have a direct line of sight to the 2 K

environment. Indeed, the choice of intercepting the thermal flux with a 4.5 K screen, and gaining the corresponding efficiency in the thermal cycle, reduces the thermal radiation load on the 2 K cold mass at negligible levels. Even with this solution, however, the thermal radiation in vacuum from the vacuum vessel inner surface to the 4.5 K shield would not be consistent with the specifications of Table 1, if not reduced further. Clearly, even considering the real emissivity of the surfaces (ranging from a few 10^{-2} of properly polished metallic surfaces to ~ 0.2 of conventional stainless steel surfaces) the radiation load would be in the hundreds of watt per meter range for the 4.5 K shield. A much better solution for this scheme is to employ a second shield at an intermediate temperature (around 70 K, practically in the range 50-80 K) and use multi-layer insulation (MLI) blankets between the shields (a series of aluminized mylar sheets separated by insulating spaces). Typical MLI performances, assuming proper handling and installation procedures reduce radiation loads to 1.2 W/m^2 from 300 K with a 30 layer blanket and 0.06 W/m^2 from 70-80 K and a 10 layer blanket. These values are achieved assuming a good insulation vacuum ($<10^{-5}$ mbar), and deteriorate by at least a factor of 20 for the case of a poor insulation vacuum of $\sim 10^{-3}$ mbar.

Finally, in the TTF cryomodule, with a two shield design and MLI insulation between the shields, the thermal radiation contribution is negligible for the 2 K environment, and amounts to 3.2 W/m , 0.14 W/m for the warm (70 K) and cold (4.5 K) shields, respectively.

Thermal design: heat conduction

The second contribution to the static loads come from the direct thermal conduction through the cold mass supports and the inserts that need to connect the cold mass to the external environment, in order to provide structural support or the necessary RF and signals communication. In the simple 1D case of the heat flow through a conducting path of surface S and length ℓ between the fixed temperatures T_1 and T_2 , we have

$$\dot{q} = -\frac{S}{\ell} \int_{T_1}^{T_2} k_{th}(T) dT$$

and k_{th} is the thermal conductivity of the material. The thermal conduction integrals among the different heat interception temperatures of the TTF cryostat for few selected representative materials are listed in Table 4.

From this table it is clear that all possible conduction paths from the external should be minimized, and the material properly chosen. In particular, the structural support of the cold mass (with a weight slightly less than 3000 kg, i.e. a 30 kN load) needs to be realized with a minimal heat load on the 2 K bath and in a reasonable space ($< 0.15 \text{ m}$, in order not to increase the module cross section). As an example we can try to see the effect of using two materials: stainless steel and a fibreglass composite material (G10), assuming conservative design stresses of 100 and 40 MPa, respectively.

Table 4: Thermal conduction integrals for selected representative materials and different temperature ranges.

Thermal conduction integral: 2 to 4.5 K [W/m]	
G10 composite	0.134
Steel	0.453
Aluminum (6061)	19.3
Copper	471
Thermal conduction integral: 4.5 K to 70 K [W/m]	
G10 composite	16.8
Steel	270
Aluminum (6061)	5000
Copper	55000
Thermal conduction integral: 70 K to 300 K [W/m]	
G10 composite	150
Steel	2800
Aluminum (6061)	31300
Copper	93700

This simple exercise leads to a support transverse section of:

$$S_{ss} = \frac{30000 \text{ N}}{10^8 \text{ Pa}} = 3 \cdot 10^{-4} \text{ m}^2$$

$$S_{G10} = \frac{30000 \text{ N}}{4 \cdot 10^7 \text{ Pa}} = 7.5 \cdot 10^{-4} \text{ m}^2$$

assuming no heat interception and the minimal section, to a minimal conduction load at 2 K (see Table 4) of

$$\dot{q}_{SS} = 3070 \cdot 3 \cdot 10^{-4} / 0.15 \approx 6 \text{ W}$$

$$\dot{q}_{G10} = 167 \cdot 7.5 \cdot 10^{-4} / 0.15 \approx 0.8 \text{ W}$$

Clearly, the use of a reduced conduction material improves the impact on the thermal load nearly by an order of magnitude.

A further optimization can be performed by intercepting the heat flux at the 70 K and 4.5 heat sinks provided by the shields, resulting in the final TTF configuration, which uses a 140 mm long G10 pipe with a diameter of 300 mm and a wall thickness of 2.2 mm. Finally we have a load of 0.04 W at 2 K, 0.8 W at 4.5 K and 10 W at 70 K per support post.

Similarly, using a thin copper layer, for RF purposes, deposited on a steel outer conductor, the conduction heat load for the couplers can be assessed, and the final result is presented in Table 5.

Result of the static budget

As a summary of the design procedure described above, in Table 5 we report the summary of the estimated static losses in the various cryogenic circuits for the 3rd generation of the module, with a breakdown in the main contributors. A deeper discussion can be found in the TTF CDR [8] and the TESLA TDR [9].

Note that the largest contribution to the low temperature heat loads in Table 5 is given by the relatively large amount of cables planned for the large amount of diagnostics foreseen in the first cryomodule prototypes.

Table 5: Static heat load budget for TTF CRY3.

2 K losses	~ 2.8 W
Radiation from 4.5 K shield	-
3 Support Posts	0.12 W
8 Couplers	0.24 W
Cabling (TTF-CDR)	2.40 W
4.5 K losses	~ 11.4 W
Radiation from 70 K shield	1.68 W
3 Support Posts	2.40 W
8 Couplers	2.52 W
HOM absorbers	1.20 W
Power and cabling	3.60 W
70 K losses	~ 93 W
Radiation from vacuum vessel	38 W
3 Support Posts	30 W
8 Couplers	18 W
Power and cabling	7 W

Cryogenics: the dynamic load

In addition to the static heat loads, which can be minimized by the design techniques described in the previous paragraphs, the cryogenics of the module (i.e. piping sizes, cooling requirements) need to take into account the amount of RF power deposited in the 2 K bath by the cavities (which depends on the quality factor of the resonator and on the geometrical R/Q parameter, in addition to the RF duty cycle) and on the power intercepted by the heat sinks at 4.5 K and 70 K for the main coupler and HOM couplers/absorbers thermalization.

Details of the full heat loss budgets, including dynamic loads, for a variety of beam structure and cavity gradients scenarios can be found in the TTF-CDR and TESLA-TDR.

Long Cryomodules: supporting the cold mass

As it was mentioned in the previous paragraphs, the cold mass hangs from the vacuum vessel, supported by three posts, made of G10 fibreglass composite material. The central post is longitudinally fixed to the vacuum vessel, whereas the two lateral posts can slide longitudinally, in order to accommodate the longitudinal movements during the cooldown and warmup of the cold mass.

The longitudinal cavity positioning in the module is achieved through an invar rod (with a relatively small thermal contraction, as shown in Table 2), at which the cavities are connected at the coupler side (the coupler position is determined at the warm temperature port on the vacuum vessel).

The cavities can then slide longitudinally with respect to the steel HeGRP and their longitudinal position is then independent from the huge contraction of the 12 m long supporting pipe.

The sliding connection is achieved through rolling needles, which reduce the friction between the Ti pads welded on the He tank and the C shaped clamps supporting the cavities to the HeGRP. Adjustable screws

and spring washers allow the cavity horizontal and vertical centering. Details of the low friction sliding supports are shown in Figure 7.

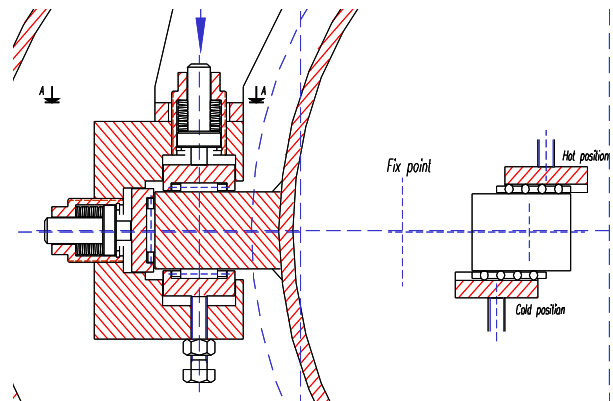


Figure 7: The low friction sliding cavity support, used to decouple the longitudinal cavity position from the shrinkage of the steel HeGRP.

Design iterations for fabrication, alignment, referencing, assembly and operation

Three design iterations have been performed on the TTF cryomodules since the original pre-prototype installed and tested in 1997. Mainly, the iterations were needed either to simplify the fabrication and assembly procedures (e.g. smaller shield segments, finger welding schemes for integrating the cooling piping in the shields, simplified thermal shield cones and braids at the couplers) and to set a reliable strategy for achieving the alignment tolerances of the active elements with the proper definition of reference surfaces and positions.

The main change in the second generation was the direct integration of the cooling pipes for the shields, which allowed to reduce the large number of expensive and unreliable copper braids used in CRY1. The specially shaped cooling pipes are directly welded to the shield component, by means of stress-relieving fingers.

This redesign of the cooling scheme for the cold mass allowed to minimize the maximum temperature gradients within the shields during the cold mass cooldown. Thermal gradients less than 60 K develop along the structure for a linear cooldown rate of 12 hours, leading to tolerable stresses [12].

Figure 8 shows a picture of the temperature field in the shields from finite element coupled thermo-structural simulations at the moment where the maximal thermal gradient is developed. The maximum gradient is concentrated in the welding regions, where the fingers unload the structure.

With the third (and last) generation, CRY3, the components in the entire cross section were redistributed in order to use a standard, 150 mm smaller diameter, “pipeline” tube for the vacuum vessel size (38”).

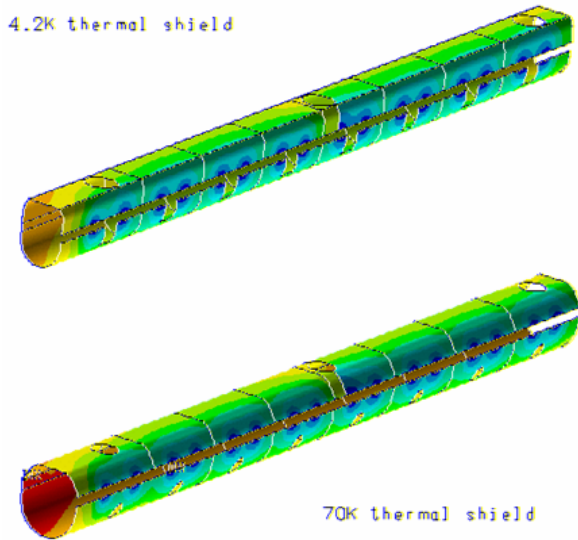


Figure 8: Temperature distribution in the shields at the maximum gradient during the cooldown.

The success of the design iteration in improving the performances of the modules in terms of alignment of the active elements were made possible by the on line monitoring of the cold mass movements during the cooldown, warmup and operation of the modules [13]. All cryomodules were equipped with (at least) one stretched wire, suspended at the room temperature regions in the module end/feed caps, and many Wire Position Monitors (WPM) stripline sensors connected to the cold mass, providing a measure of the relative displacement between the wire and the cold mass. This instrumentation allowed monitoring the cold mass deformation due to the asymmetrical forces at the module ends in the first prototypes and its minimization in CRY3. Figure 9 shows that the achievement of the reproducibility of the cold mass position at 2 K between two successive cooldowns, within the TTF specifications. Recently the electronic front end of the WPM diagnostics has been extended to include the capability of low frequency (<100 Hz) vibrations of the cold mass.

Detailed measurements of the static heat losses of the CRY3 modules in the TTF linac have been performed and agree consistently with the design estimation, and are shown in Table 6. We note that these values include the cryogenic end and feed cap of the two module string.

CONCLUSIONS

SRF cryomodules are extremely complex systems, and their design optimization is strongly dependent on the accelerator application for which they are intended. The TTF/TESLA cryomodule is a recent example of the emerging practice of an integrated design which takes into account the overall accelerator optimization. The TTF module design is currently the baseline for the future large size SRF linac programs, like the XFEL at DESY and the International Linear Collider.

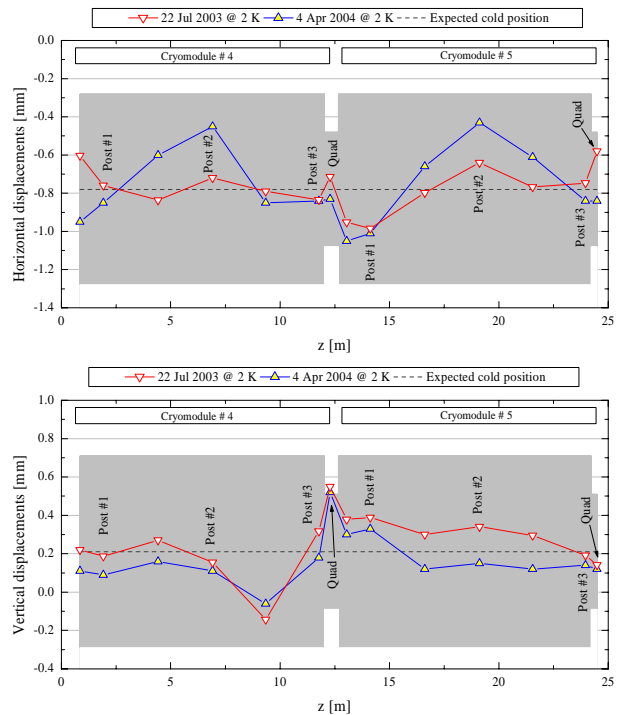


Figure 9: Reproducibility of the horizontal (top) and vertical (bottom) position of the cold mass between two successive cooldowns, as measured from the WPM line in modules 4 and 5 of the TTF linac. The gray area represent the active elements alignment specification.

Table 6: Measured static losses in the linac.

Measured static losses (including caps)	[W]
2 K circuit	<3.5
4.3 K circuit	13
40/80 K circuit	74

REFERENCES

- [1] K.W. Shepard et al., IEEE Trans. Nucl. Sci, 24 (1977), p. 1147.
- [2] S. Takeuchi, Proceedings of the 3rd Workshop on RF Superconductivity, Argonne, (1988), p. 55.
- [3] G. Fortuna et al., Proceedings of the 3rd Workshop on RF Superconductivity, Argonne, (1988), p. 399.
- [4] M. Pekeler et al., Development of a Superconducting RF Module for Acceleration of Protons and Deuterons at Very Low Energy, in Proceedings of HPSL2005, NIU Naperville.
- [5] R. Sundelin et al., IEEE Trans Nucl. Sci, 32 (1985), p. 3570.
- [6] G.Geshonke, in Proceedings of the 7th Workshop on RF Superconductivity, France (1995) p. 143.
- [7] J. Preble, in Proceedings of the 7th Workshop on RF Superconductivity, France (1995) p. 173.
- [8] D.A. Edwards (ed), TESLA Test Facility Linac Design Report, DESY Print, March 1995, TESLA 95-01.
- [9] TESLA Technical Design Report, Part II: The Accelerator, March 2001, DESY 2001-011, ECFA

2001-209, TESLA Report 2001-23, TESLA-FEL
2001-05.

- [10] C. Pagani et al., Construction, Commissioning and Cryogenic Performances of the First TESLA Test Facility (TTF) Cryomodule, *Advances in Cryogenic Engineering*, Vol 43, 1998, p. 87.
- [11] J.G. Weisend II et al., The TESLA Test Facility (TTF) Cryomodule: A Summary of Work to Date, *Advances in Cryogenic Engineering*, Vol 45, 2000, p. 825.
- [12] D. Barni et al., Cooldown Simulations for TESLA Test Facility (TTF) Cryostats, *Advances in Cryogenic Engineering*, Vol 43, 1998, p. 315.
- [13] A. Bosotti et al., Analysis of the Cold Mass Displacements at the TTF, *Proceedings of EPAC 2004*, Lucerne, Switzerland, p. 1681.